



Eshelby tensors for an ellipsoidal inclusion in a micropolar material

Hansong Ma ^a, Gengkai Hu ^{a,b,*}

^a *Department of Applied Mechanics, Beijing Institute of Technology, Beijing 100081, China*

^b *National Key Lab for the Prevention and Control of Explosion Disaster, BIT, Beijing 100081, China*

Received 21 January 2005; received in revised form 13 December 2005; accepted 13 December 2005

Available online 3 July 2006

Abstract

Micropolar Eshelby tensors for an ellipsoidal inclusion are derived in an analytical form, which involves only one-dimensional integral. The numerical evaluation of the Eshelby tensors are also performed, it is found that the micropolar Eshelby tensors are not uniform in the ellipsoidal inclusion, however, their variations over the ellipsoidal domain are not significant. When size of inclusion is large compared to the characteristic length of the micropolar material, the micropolar Eshelby tensor is reduced to the classical one. It is also demonstrated that for a general ellipsoidal inclusion a uniform eigenstrain or eigentorsion produces on average only nonzero strain or torsion, and the average Eshelby relations are uncoupled.

© 2006 Elsevier Ltd. All rights reserved.

Keywords: Eshelby tensor; Micropolar; Ellipsoidal inclusion

1. Introduction

Material is endowed with microstructure, like atoms and molecules at microscopic scale, grains and fibers or particulates at mesoscopic scale. Homogenization of a basically heterogeneous material depends on scale of interest. When stress fluctuation is small enough compared to microstructure of material, homogenization can be made without considering the detailed microstructure of the material. However, if it is not the case, the microstructure of material must be considered properly in a homogenized formulation [1,2]. The concept of microcontinuum, proposed by Eringen [1], can take into account the microstructure of material while the theory itself remains still in a continuum formulation. The first grade microcontinuum consists a hierarchy of theories, such as, micropolar, microstretch and micromorphic, depending on how much micro-degrees of freedom are incorporated. These microcontinuum theories are believed to be potential tools to characterize the behavior of material with complicated microstructures.

* Corresponding author. Address: Department of Applied Mechanics, Beijing Institute of Technology, Beijing 100081, China. Fax: +86 10 68914780.

E-mail address: hugeng@public.bta.net.cn (G. Hu).

The most popular microcontinuum theory is micropolar one, in this theory a material point can still be considered as infinitely small, however, there are microstructures inside of this point. So there are two sets of variable to describe the deformation of this material point, one characterizes the motion of the inertia center of this material point; the other describes the motion of the microstructure inside of this point. In micropolar theory, the motion of the microstructure is supposed to be an independently rigid rotation. Application of this theory can be found in Refs. [1,3]. The inclusion problem for a micropolar medium is firstly addressed by Cheng and He [4,5] with help of Green's function technique. In their work an eigentorsion was introduced in addition to the classical eigenstrain introduced by Eshelby [6], four Eshelby tensors are then introduced for an inclusion in a micropolar material. Cheng and He [4,5] derived the analytical expressions of these four Eshelby tensors for a spherical inclusion and a cylindrical inclusion, respectively. The results show that even for the simplest inclusion shape (for example a sphere), the Eshelby tensors are not uniform inside of the inclusion.

Based on the Eshelby relations for a micropolar material, Xun et al. [7], Liu and Hu [8], and Hu et al. [2] have proposed an analytical homogenization method for micropolar composites, the influence of particle size on the elastoplastic behavior of the composites can be successfully predicted. However, Eshelby tensors for a general ellipsoidal inclusion are not available at present, the influence of fiber's shape and size on overall elastoplastic behavior for micropolar composites has not been addressed yet. The objective of this paper is to derive the Eshelby tensors for a general ellipsoidal inclusion, these Eshelby tensors are essential to predict overall behavior of micropolar composites. The manuscript is arranged as follows, in Section 2, a brief theory for a micropolar material will be recalled; in Section 3, analytical expressions of Eshelby tensors for a general ellipsoidal inclusion will be derived, the characteristic of the derived Eshelby tensors and their average over the ellipsoidal domain will be examined in Section 4. Index notation for a tensor (or vector) is adopted in this paper, except some vector representations appear in bold letter as used for convenience.

2. Basic equations for a micropolar material

For a micropolar body, the governing equations are given by Eringen [1] and Nowacki [9]:

$$\varepsilon_{ij} = u_{j,i} - e_{kij}\varphi_k, \quad \kappa_{ij} = \varphi_{j,i} \quad (1a)$$

$$\sigma_{ij,i} + f_j = 0, \quad m_{ij,i} + e_{jik}\sigma_{ik} + l_j = 0 \quad (1b)$$

$$\sigma_{ji} = C_{jikl}\varepsilon_{kl} + B_{jikl}\kappa_{kl}, \quad m_{ji} = B_{jikl}\varepsilon_{kl} + D_{jikl}\kappa_{kl} \quad (1c)$$

where σ_{ij} and m_{ij} denote the stress and couple stress tensors, ε_{ij} and κ_{ij} are the strain and torsion tensors, u_i and φ_i are the displacement and microrotation vectors, respectively. C_{ijkl} , B_{ijkl} and D_{ijkl} are the elasticity tensors of the micropolar material, e_{ijk} is permutation tensor. f_j and l_j are the body force and body torque, separately.

In particular, for a centrosymmetric and isotropic micropolar body, the elasticity tensors are specified as [9]:

$$B_{ijkl} = 0 \quad (2a)$$

$$C_{jikl} = \lambda\delta_{ij}\delta_{kl} + (\mu + \kappa)\delta_{jk}\delta_{il} + (\mu - \kappa)\delta_{ik}\delta_{jl} \quad (2b)$$

$$D_{jikl} = \alpha\delta_{ij}\delta_{kl} + (\beta + \gamma)\delta_{jk}\delta_{il} + (\beta - \gamma)\delta_{ik}\delta_{jl} \quad (2c)$$

where μ, λ are the classical Lamé's constants and $\kappa, \gamma, \beta, \alpha$ are the new elastic constants introduced in micropolar theory.

Eq. (1) can be further arranged in the following form with the two basic variables u_i, ϕ_i

$$C_{jikl}u_{l,kj} + 2\kappa e_{ijk}\varphi_{k,j} + f_i = 0 \quad (3a)$$

$$D_{jikl}\varphi_{l,kj} - 4\kappa\varphi_i + 2\kappa e_{ijk}u_{k,j} + l_i = 0 \quad (3b)$$

Four Green's functions G_{ln} , \widehat{G}_{ln} , Φ_{ln} and $\widehat{\Phi}_{ln}$ for a micropolar material can be derived by solving the following equations:

$$C_{jikl}G_{ln,kj} + 2\kappa e_{ijl}\widehat{\Phi}_{ln,j} + \delta_{in}\delta(\mathbf{x} - \mathbf{x}') = 0, \quad D_{jikl}\Phi_{ln,kj} - 4\kappa\Phi_{in} + 2\kappa e_{ijl}G_{ln,j} = 0 \quad (4a)$$

$$C_{jikl}\widehat{G}_{ln,kj} + 2\kappa e_{ijl}\widehat{\Phi}_{ln,j} = 0, \quad D_{jikl}\widehat{\Phi}_{ln,kj} - 4\kappa\widehat{\Phi}_{in} + 2\kappa e_{ijl}\widehat{G}_{ln,j} + \delta_{in}\delta(\mathbf{x} - \mathbf{x}') = 0 \quad (4b)$$

where δ_{ij} is the Kronecker-delta function, and $\delta(\mathbf{x} - \mathbf{x}')$ is one-dimensional Dirac-delta function. The analytical expressions of Green's functions for an infinite centrosymmetric and isotropic micropolar body have been provided by Sandru [10], and they are listed in Appendix.

3. Inclusion problem for a micropolar medium

Considering an inclusion Ω in an infinite centrosymmetric and isotropic micropolar material, a uniform asymmetric eigenstrain $\boldsymbol{\varepsilon}^*$ and an eigentorsion $\boldsymbol{\kappa}^*$ are prescribed in the inclusion. Here the inclusion means that its material constants are the same as the surrounding matrix, as introduced by Mura [11]. It can be shown that the effect of the eigenstrain and eigentorsion can be simulated by a distributed body force and body torque, and further with help of Green's functions for the micropolar material, the induced displacement and rotation in the micropolar medium due to the prescribed eigenstrain and eigentorsion in the inclusion can be expressed as

$$u_n(\mathbf{x}) = - \int_V (C_{lkji}\varepsilon_{ji}^* G_{kn,l} + 2\kappa e_{ijk}\varepsilon_{ji}^* \Phi_{kn} - D_{lkji}\kappa_{ji}^* \Phi_{kn,l}) d\mathbf{x}' \tag{5a}$$

$$\varphi_n(\mathbf{x}) = \int_V (C_{lkji}\varepsilon_{ji}^* \widehat{G}_{kn,l} + 2\kappa e_{ijk}\varepsilon_{ji}^* \widehat{\Phi}_{kn} - D_{lkji}\kappa_{ji}^* \widehat{\Phi}_{kn,l}) d\mathbf{x}' \tag{5b}$$

Differentiating the both sides of Eq. (5), the induced strain and torsion by the prescribed eigenstrain and eigentorsion can be written as [5]

$$\boldsymbol{\varepsilon}(\mathbf{x}) = \mathbf{K}(\mathbf{x}) : \boldsymbol{\varepsilon}^* + \mathbf{L}(\mathbf{x}) : \boldsymbol{\kappa}^* \tag{6a}$$

$$\boldsymbol{\kappa}(\mathbf{x}) = \widehat{\mathbf{K}}(\mathbf{x}) : \boldsymbol{\varepsilon}^* + \widehat{\mathbf{L}}(\mathbf{x}) : \boldsymbol{\kappa}^* \tag{6b}$$

where

$$K_{mnji}(\mathbf{x}) = I_{nji,m}^S(\mathbf{x}) + I_{nji,m}(\mathbf{x}) - e_{lmn}\widehat{I}_{lji}(\mathbf{x}) \tag{7a}$$

$$L_{mnji}(\mathbf{x}) = J_{nji,m}(\mathbf{x}) - e_{lmn}\widehat{J}_{lji}(\mathbf{x}) \tag{7b}$$

$$\widehat{K}_{mnji}(\mathbf{x}) = \widehat{I}_{nji,m}(\mathbf{x}) \tag{7c}$$

$$\widehat{L}_{mnji}(\mathbf{x}) = \widehat{J}_{nji,m} \tag{7d}$$

and

$$I_{nji}^S = \frac{\lambda + \mu}{\lambda + 2\mu} \psi_{,ijn}(\mathbf{x}) - \frac{\lambda}{\lambda + 2\mu} \delta_{ij}\phi_{,n}(\mathbf{x}) - \delta_{in}\phi_{,j}(\mathbf{x}) - \delta_{jn}\phi_{,i}(\mathbf{x}) \tag{8a}$$

$$I_{nji} = 2\mu H[h^2\phi_{,ijn}(\mathbf{x}) - h^2M_{,ijn}(\mathbf{x}, h) + \delta_{jn}M_{,i}(\mathbf{x}, h)] \tag{8b}$$

$$\begin{aligned} J_{nji}(\mathbf{x}) = & -\frac{1}{2\mu} [(\beta + \gamma)e_{nik}\phi_{,jk}(\mathbf{x}) + (\beta - \gamma)e_{nj\kappa}\phi_{,ik}(\mathbf{x})] \\ & + \frac{1}{2\mu} [(\beta + \gamma)e_{nik}M_{,jk}(\mathbf{x}, h) + (\beta - \gamma)e_{nj\kappa}M_{,ik}(\mathbf{x}, h)] \\ & - \frac{\alpha}{2\mu} \delta_{ji}e_{nkl}[\phi_{,kl} - M_{,kl}(\mathbf{x}, h)] \end{aligned} \tag{8c}$$

$$\begin{aligned} \widehat{I}_{nji}(\mathbf{x}) = & -\frac{1}{2\mu} [\lambda\delta_{ji}e_{nkl}\phi_{,kl}(\mathbf{x}) + \kappa e_{jik}\phi_{,kn}(\mathbf{x}) + (\mu + \kappa)e_{ink}\phi_{,kj}(\mathbf{x}) + (\mu - \kappa)e_{jnk}\phi_{,ki}(\mathbf{x})] \\ & + \frac{1}{2\mu} [\lambda\delta_{ji}e_{nkl}M_{,kl}(\mathbf{x}, h) + (\mu + \kappa)e_{jik}M_{,kn}(\mathbf{x}, h) + (\mu + \kappa)e_{ink}M_{,kj}(\mathbf{x}, h) \\ & + (\mu - \kappa)e_{jnk}M_{,ki}(\mathbf{x}, h)] + \frac{1}{2} e_{jik}M_{,kn}(\mathbf{x}, g) - \frac{\mu + \kappa}{2\mu h^2} e_{nji}M(\mathbf{x}, h) \end{aligned} \tag{8d}$$

$$\begin{aligned} \widehat{J}_{nji}(\mathbf{x}) = & -\frac{\beta}{2\mu} \phi_{,ijn}(\mathbf{x}) + \frac{\mu + \kappa}{4\mu\kappa} [\alpha\delta_{ij}M_{,kkn}(\mathbf{x}, h) + 2\beta M_{,ijn}(\mathbf{x}, h)] - \frac{1}{4\kappa} [\alpha\delta_{ij}M_{,kkn}(\mathbf{x}, g) + 2\beta M_{,ijn}(\mathbf{x}, g)] \\ & - \frac{\mu + \kappa}{4\mu\kappa h^2} [\alpha\delta_{ij}M_{,n}(\mathbf{x}, h) + (\beta + \gamma)\delta_{in}M_{,j}(\mathbf{x}, h) + (\beta - \gamma)\delta_{jn}M_{,i}(\mathbf{x}, h)] \end{aligned} \tag{8e}$$

The constants introduced in Eq. (8) are defined by

$$H = \kappa/[\mu(\mu + \kappa)], \quad h^2 = \frac{(\mu + \kappa)(\gamma + \beta)}{4\mu\kappa}, \quad g^2 = \frac{(\alpha + 2\beta)}{4\kappa} \tag{9}$$

The tensors $\mathbf{K}, \widehat{\mathbf{K}}, \mathbf{L}, \widehat{\mathbf{L}}$ are called micropolar Eshelby tensors [5]. It can be seen from Eqs. (6)–(8) that computation of the micropolar Eshelby tensors depends on the following three potential functions and their derivatives, which are defined by

$$\psi(\mathbf{x}) = \frac{1}{4\pi} \int_{\Omega} r \, d\mathbf{x}', \quad \phi(\mathbf{x}) = \frac{1}{4\pi} \int_{\Omega} \frac{1}{r} \, d\mathbf{x}', \quad M(\mathbf{x}, k) = \frac{1}{4\pi} \int_{\Omega} \frac{e^{-r/k}}{r} \, d\mathbf{x}' \tag{10}$$

where $r = |\mathbf{x} - \mathbf{x}'|$.

The first and second integrals appeared in Eq. (10) are the same as in classical Eshelby tensor [11], and they have been evaluated analytically by Eshelby [6] for a general ellipsoidal inclusion. Therefore, the key point for evaluating the micropolar Eshelby tensors is to calculate the last integral in Eq. (10) for a general ellipsoidal inclusion.

For a spherical and cylindrical inclusions, the last integral has been provided analytically by Cheng and He [4,5]. For a general ellipsoidal inclusion, this integral cannot be evaluated in a fully analytical form, however, we will reduce this integral as simple as possible, this effort is believed to be useful for further micromechanical modeling.

Following Michelitsch et al. [12], after some mathematical algebra, the potential $M(\mathbf{x}, k)$ can be reduced to the following form, involving only one-dimensional integral for a general ellipsoidal inclusion:

$$M(\mathbf{x}, k) = \frac{1}{4\pi} \int_{\Omega} \frac{e^{-r/k}}{r} \, d\mathbf{x}' = k^2 - k^2 \frac{a_3}{2} \int_0^{\infty} (D \cdot A) \, du \tag{11}$$

where the constants in Eq. (11) are defined as

$$D = \frac{1}{(u + a_3^2)^{3/2}} \left(1 + \frac{a}{k} \sqrt{\frac{u + a_3^2}{u + a^2}} \right) \exp \left(-\frac{a}{k} \sqrt{\frac{u + a_3^2}{u + a^2}} \right),$$

$$A = I_0(B\rho) \cosh(Cz), \quad B = \frac{1}{k} \sqrt{\frac{u}{u + a^2}}, \quad C = \frac{a}{k\sqrt{u + a^2}},$$

$$u = a_3^2 \tan^2 \theta, \quad \rho = \sqrt{x_1^2 + x_2^2}$$

I_M is the M th order modified Bessel function of the first kind, a is the half short axis of the ellipsoid and a_3 is its half major axis, the major axis of the ellipsoid lines with the axis z .

The derivatives of Eq. (11) are given by

$$M_{,i}(\mathbf{x}, k) = -\frac{a_3}{2} k^2 \int_0^{\infty} (D \cdot A_{,i}) \, du \tag{12a}$$

$$M_{,ij}(\mathbf{x}, k) = -\frac{a_3}{2} k^2 \int_0^{\infty} (D \cdot A_{,ij}) \, du \tag{12b}$$

$$M_{,ijm}(\mathbf{x}, k) = -\frac{a_3}{2} k^2 \int_0^{\infty} (D \cdot A_{,ijm}) \, du \tag{12c}$$

$$M_{,ijmn}(\mathbf{x}, k) = -\frac{a_3}{2} k^2 \int_0^{\infty} (D \cdot A_{,ijmn}) \, du \tag{12d}$$

where

$$A_{,x} = B \cosh(Cz) I_1(B\rho) \frac{x_x}{\rho}$$

$$A_{,x\beta} = B \cosh(Cz) \frac{1}{2\rho^3} [B\rho [I_0(B\rho) + I_2(B\rho)] x_x x_\beta + 2I_1(B\rho) (\rho^2 \delta_{x\beta} - x_x x_\beta)]$$

$$\begin{aligned}
 A_{,\alpha\beta\gamma} &= B \cosh(Cz) \cdot \left\{ \left[-\frac{3B}{2\rho^4} x_\alpha x_\beta x_\gamma + \frac{B}{2\rho^2} (\delta_{\alpha\beta} x_\gamma + \delta_{\alpha\gamma} x_\beta + \delta_{\gamma\beta} x_\alpha) \right] I_0(B\rho) \right. \\
 &+ \left[\frac{3}{\rho^5} x_\alpha x_\beta x_\gamma + \frac{3B^2}{4\rho^3} x_\alpha x_\beta x_\gamma - \frac{1}{\rho^3} (\delta_{\alpha\beta} x_\gamma + \delta_{\alpha\gamma} x_\beta + \delta_{\gamma\beta} x_\alpha) \right] I_1(B\rho) \\
 &+ \left. \left[-\frac{3B}{2\rho^4} x_\alpha x_\beta x_\gamma + \frac{B}{2\rho^2} (\delta_{\alpha\beta} x_\gamma + \delta_{\alpha\gamma} x_\beta + \delta_{\gamma\beta} x_\alpha) \right] I_2(B\rho) + \left[\frac{B^2}{4\rho^3} x_\alpha x_\beta x_\gamma \right] I_3(B\rho) \right\} \\
 A_{,\alpha\beta\gamma\lambda} &= B \cosh(Cz) \cdot \left\{ \frac{B}{\rho^6} \left[\frac{15}{2} x_\alpha x_\beta x_\gamma x_\lambda + \frac{3}{8} B^2 \rho^2 x_\alpha x_\beta x_\gamma x_\lambda - \frac{3}{2} \rho^2 x_\lambda (\delta_{\alpha\beta} x_\gamma + \delta_{\alpha\gamma} x_\beta + \delta_{\gamma\beta} x_\alpha) \right. \right. \\
 &- \frac{3}{2} \rho^2 (\delta_{\alpha\lambda} x_\beta x_\gamma + \delta_{\beta\lambda} x_\alpha x_\gamma + \delta_{\gamma\lambda} x_\beta x_\alpha) + \frac{\rho^4}{2} (\delta_{\alpha\beta} \delta_{\gamma\lambda} + \delta_{\alpha\gamma} \delta_{\beta\lambda} + \delta_{\alpha\lambda} \delta_{\gamma\beta}) \left. \right] I_0(B\rho) \\
 &+ \frac{1}{\rho^7} \left[-\frac{9}{2} B^2 \rho^2 x_\alpha x_\beta x_\gamma x_\lambda - 15 x_\alpha x_\beta x_\gamma x_\lambda + \frac{3}{4} B^2 \rho^4 x_\lambda (\delta_{\alpha\beta} x_\gamma + \delta_{\alpha\gamma} x_\beta + \delta_{\gamma\beta} x_\alpha) \right. \\
 &+ 3 \rho^2 x_\lambda (\delta_{\alpha\beta} x_\gamma + \delta_{\alpha\gamma} x_\beta + \delta_{\gamma\beta} x_\alpha) + 3 \rho^2 (\delta_{\alpha\lambda} x_\beta x_\gamma + \delta_{\beta\lambda} x_\alpha x_\gamma + \delta_{\gamma\lambda} x_\beta x_\alpha) \\
 &+ \left. \frac{3}{4} B^2 \rho^4 (\delta_{\alpha\lambda} x_\beta x_\gamma + \delta_{\beta\lambda} x_\alpha x_\gamma + \delta_{\gamma\lambda} x_\beta x_\alpha) - \rho^4 (\delta_{\alpha\beta} \delta_{\gamma\lambda} + \delta_{\alpha\gamma} \delta_{\beta\lambda} + \delta_{\alpha\lambda} \delta_{\gamma\beta}) \right] I_1(B\rho) \\
 &+ \frac{B}{\rho^6} \left[\frac{15}{2} x_\alpha x_\beta x_\gamma x_\lambda + \frac{B^2 \rho^2}{2} x_\alpha x_\beta x_\gamma x_\lambda - \frac{3}{2} \rho^2 x_\lambda (\delta_{\alpha\beta} x_\gamma + \delta_{\alpha\gamma} x_\beta + \delta_{\gamma\beta} x_\alpha) \right. \\
 &- \left. \frac{3}{2} \rho^2 (\delta_{\alpha\lambda} x_\beta x_\gamma + \delta_{\beta\lambda} x_\alpha x_\gamma + \delta_{\gamma\lambda} x_\beta x_\alpha) + \frac{\rho^4}{2} (\delta_{\alpha\beta} \delta_{\gamma\lambda} + \delta_{\alpha\gamma} \delta_{\beta\lambda} + \delta_{\alpha\lambda} \delta_{\gamma\beta}) \right] I_2(B\rho) \\
 &+ \frac{B^2}{\rho^5} \left[-\frac{3}{2} x_\alpha x_\beta x_\gamma x_\lambda + \frac{\rho^2}{4} x_\lambda (\delta_{\alpha\beta} x_\gamma + \delta_{\alpha\gamma} x_\beta + \delta_{\gamma\beta} x_\alpha) + \frac{\rho^2}{4} (\delta_{\alpha\lambda} x_\beta x_\gamma + \delta_{\beta\lambda} x_\alpha x_\gamma + \delta_{\gamma\lambda} x_\beta x_\alpha) \right] I_3(B\rho) \\
 &+ \left. \frac{B^3}{\rho^4} \left[\frac{1}{8} x_\alpha x_\beta x_\gamma x_\lambda \right] I_4(B\rho) \right\}
 \end{aligned}$$

The symbols $\alpha, \beta, \gamma, \lambda$ range from 1 to 2 and

$$\begin{aligned}
 A_{,z} &= C \sinh(Cz) I_0(B\rho) \\
 A_{,zz} &= C^2 \cosh(Cz) I_0(B\rho), \quad A_{,\alpha z} = (A_{,\alpha})_{,z} \\
 A_{,zzz} &= C^3 \sinh(Cz) I_0(B\rho), \quad A_{,\alpha zz} = (A_{,\alpha})_{,zz}, \quad A_{,\alpha\beta z} = (A_{,\alpha\beta})_{,z} \\
 A_{,zzzz} &= C^4 \cosh(Cz) I_0(B\rho), \quad A_{,\alpha zzz} = (A_{,\alpha})_{,zzz}, \quad A_{,\alpha\beta zz} = (A_{,\alpha\beta})_{,zz}, \quad A_{,\alpha\beta\gamma z} = (A_{,\alpha\beta\gamma})_{,z}
 \end{aligned}$$

With help of Eq. (12), the micropolar Eshelby tensors for an ellipsoidal inclusion can then be derived by evaluating the one-dimensional integral.

4. Numerical results

Unlike the Eshelby tensor in classical material (Cauchy medium), the micropolar Eshelby tensors are not constant inside of an ellipsoidal inclusion. So in the following, the Eshelby tensors and their averages over the ellipsoidal inclusion will be examined separately. The average Eshelby tensors are useful for determining the effective property for a micropolar composite [7,8]. In the following, we are interested only in the symmetric part K_{ijkl}^{sym} of the Eshelby tensor K_{ijkl} , defined by

$$K_{ijmn}^{sym} = \frac{1}{4} (K_{ijmn} + K_{ijnm} + K_{jimn} + K_{jinm}) \tag{13}$$

The other Eshelby tensors can be evaluated in the same way.

(a) *Eshelby tensor for an ellipsoidal inclusion:* By evaluating the integral in Eqs. (11) and (12), and with help of Eqs. (7)–(10), the Eshelby tensors for a general ellipsoidal inclusion in a micropolar medium can then be computed. In the following, we assume $l_1 = l_2 = l_3 = l$, the other material constants used in the computation

are $\lambda = 50$ Gpa, $\mu = 26$ Gpa, $\kappa = 13$ Gpa, $l = 10$ μm , respectively. Fig. 1a and b illustrates the variation of the component K_{1111}^{sym} of the Eshelby tensor for an ellipsoidal inclusion with the aspect ratio 10 on the plane $z = 0$ and on the plane $x_2 = 0$, respectively. The variations of the component K_{1122}^{sym} on the same planes are also shown in Fig. 2a and b. The size of the inclusion is set to be $a = l$. As shown in the figure, indeed the Eshelby tensors are not uniform in the ellipsoidal domain, however, their variation in the ellipsoidal inclusion is not significant. This is also checked for the other components of the Eshelby tensors.

(b) *Average Eshelby tensor for an ellipsoidal inclusion:* From Eqs. (7), (8) and (12), we find that the expressions for $\hat{\mathbf{K}}$ and \mathbf{L} have only odd order terms of the argument \mathbf{x} , so their integration over a symmetric domain vanishes. Therefore, for a general ellipsoidal inclusion, the following properties hold

$$\langle \mathbf{L} \rangle_I = 0, \quad \langle \hat{\mathbf{K}} \rangle_I = 0 \tag{14}$$

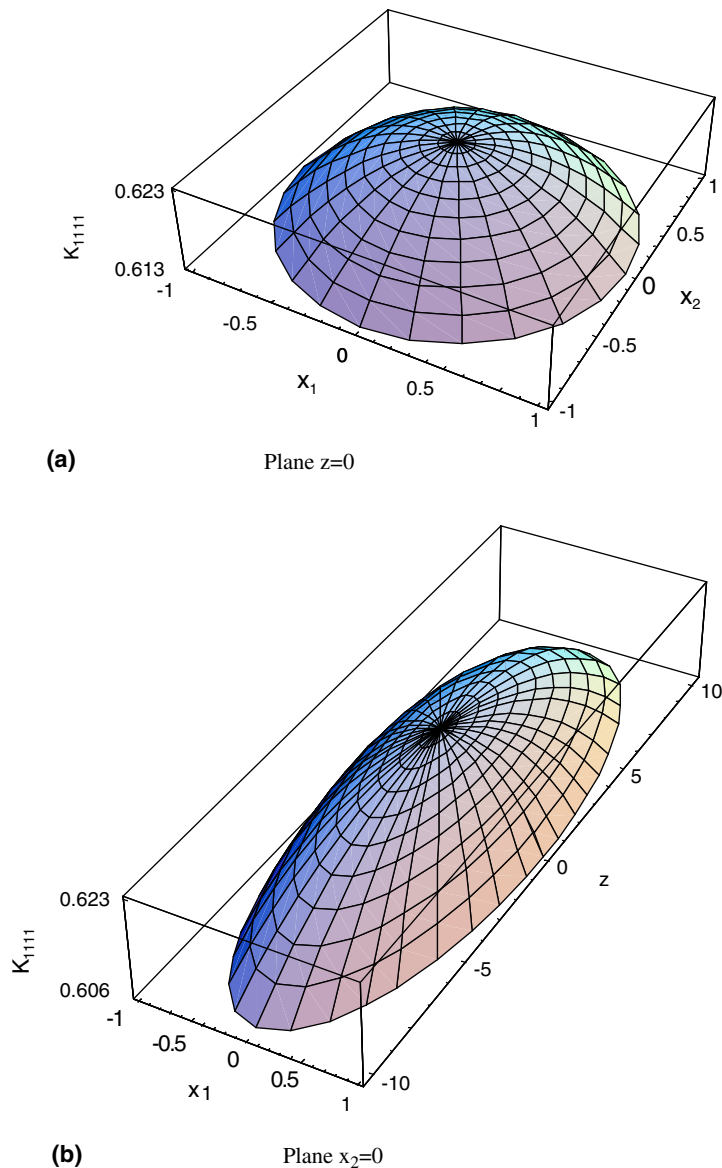


Fig. 1. Variation of component K_{1111}^{sym} of the Eshelby tensor inside of an ellipsoidal inclusion with aspect ratio 10 (a) plane $z = 0$; (b) plane $x_2 = 0$.

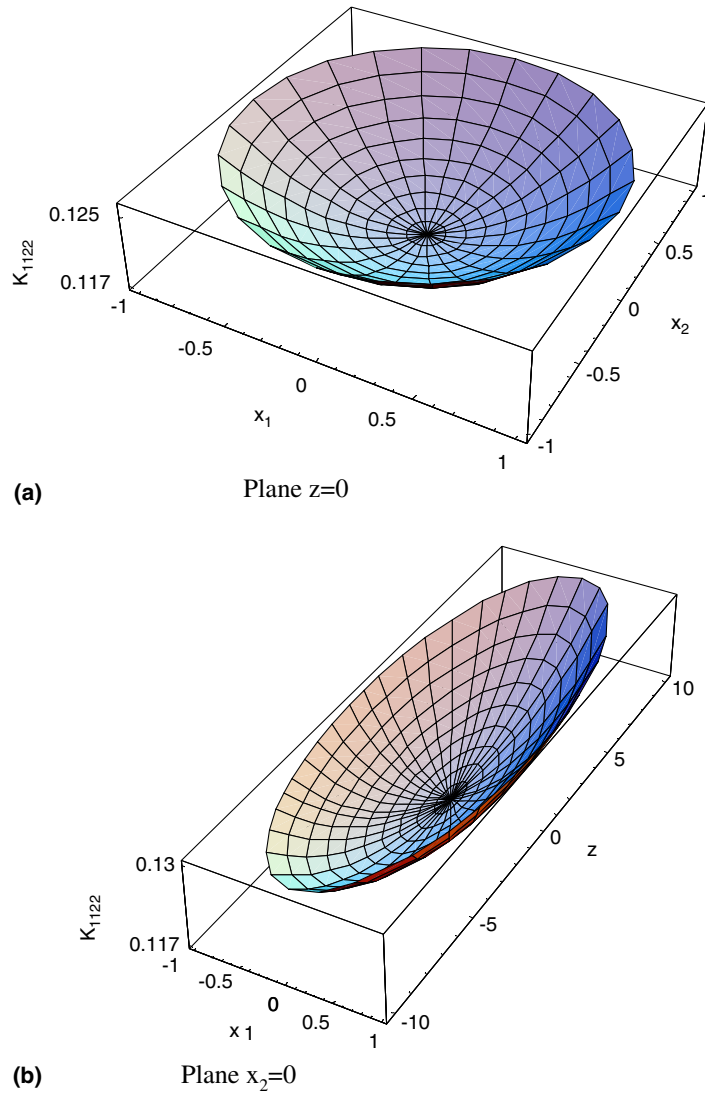


Fig. 2. Variation of component K_{1122}^{sym} of the Eshelby tensor inside of an ellipsoidal inclusion with aspect ratio 10 (a) plane $z = 0$; (b) plane $x_2 = 0$.

where $\langle \bullet \rangle_I$ means the volume average of the said quantity over the inclusion. Eq. (14) has been proven for a spherical inclusion by Liu and Hu [8].

Eq. (14) means that in the average sense, an eigenstrain only induces a nonzero average strain and an eigentorsion produces only a nonzero average torsion for a general ellipsoidal inclusion. The average Eshelby relations (Eq. (6)) are uncoupled. We will consider in the following only the average symmetric part $\langle \mathbf{K}^{sym} \rangle_I$ of the Eshelby tensor $\langle \mathbf{K} \rangle_I$, it relates the symmetric part of strain and eigenstrain by

$$\langle \boldsymbol{\varepsilon}^{sym} \rangle_I = \langle \mathbf{K}^{sym} \rangle_I : \boldsymbol{\varepsilon}^{*sym} \tag{15}$$

For a spherical and a cylindrical inclusion, $\langle \mathbf{K}^{sym} \rangle_I$ have been evaluated analytically by Xun et al. [7] and by Liu and Hu [8], they are listed in the following for further comparison:

$$\langle K_{ijkl}^{sym}(x) \rangle_I = T_1 \delta_{ij} \delta_{kl} + T_2 (\delta_{ik} \delta_{jl} + \delta_{il} \delta_{jk}) \tag{16}$$

where for a cylindrical inclusion, indices i, j range from 1 to 2, and

$$T_1 = \frac{\lambda - \mu}{4(\lambda + 2\mu)} + \frac{\kappa}{2(\kappa + \mu)} I_1(a/h) K_1(a/h) \tag{17a}$$

$$T_2 = \frac{\lambda + 3\mu}{4(\lambda + 2\mu)} - \frac{\kappa}{2(\kappa + \mu)} I_1(a/h) K_1(a/h) \tag{17b}$$

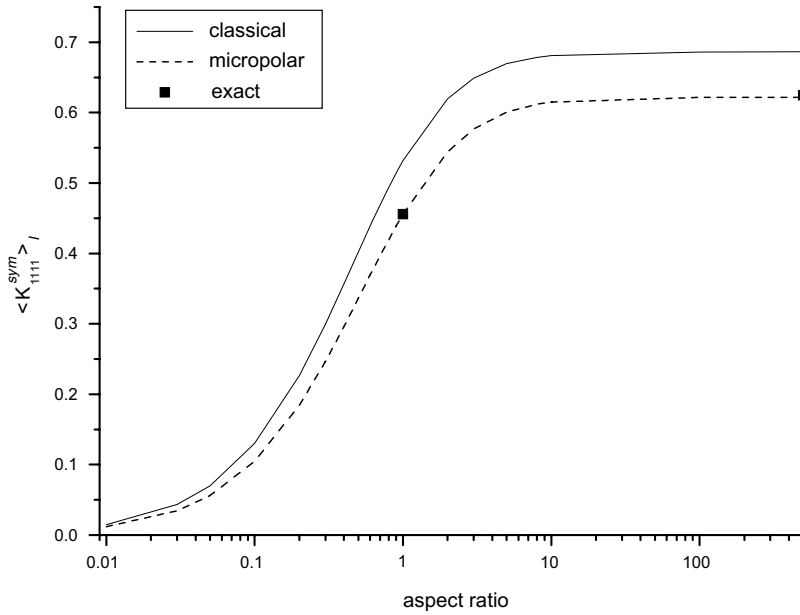


Fig. 3. Variation of component $\langle K_{1111}^{sym} \rangle_I$ of average Eshelby tensor as function of inclusion's aspect ratio.

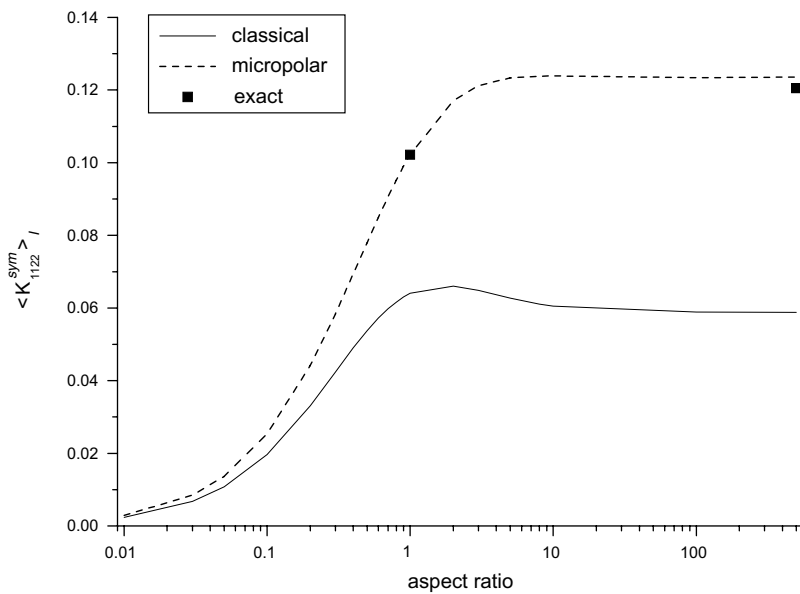


Fig. 4. Variation of component $\langle K_{1122}^{sym} \rangle_I$ of average Eshelby tensor as function of inclusion's aspect ratio.

and for a spherical inclusion, indices i, j range from 1 to 3, and

$$T_1 = \frac{3\lambda - 2\mu}{15(\lambda + 2\mu)} + \frac{2h(a+h)\kappa}{5a^3(\kappa + \mu)} \Gamma(h) \tag{18a}$$

$$T_2 = \frac{3\lambda + 8\mu}{15(\lambda + 2\mu)} - \frac{3h(a+h)\kappa}{5a^3(\kappa + \mu)} \Gamma(h) \tag{18b}$$

where a denotes the radius of the sphere or cylinder, K_1 is the first order modified Bessel function of the type II, and $\Gamma(y) = e^{-a/y}[a \cosh(a/y) - y \sinh(a/y)]$.

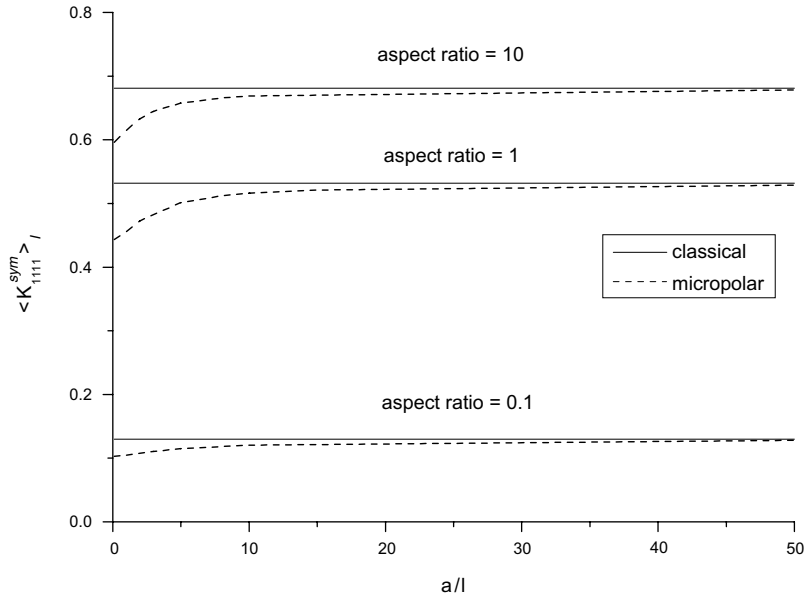


Fig. 5. Variation of component $\langle K_{1111}^{sym} \rangle / l$ of average Eshelby tensor as function of fiber size a for different aspect ratios 10, 1 and 0.1.

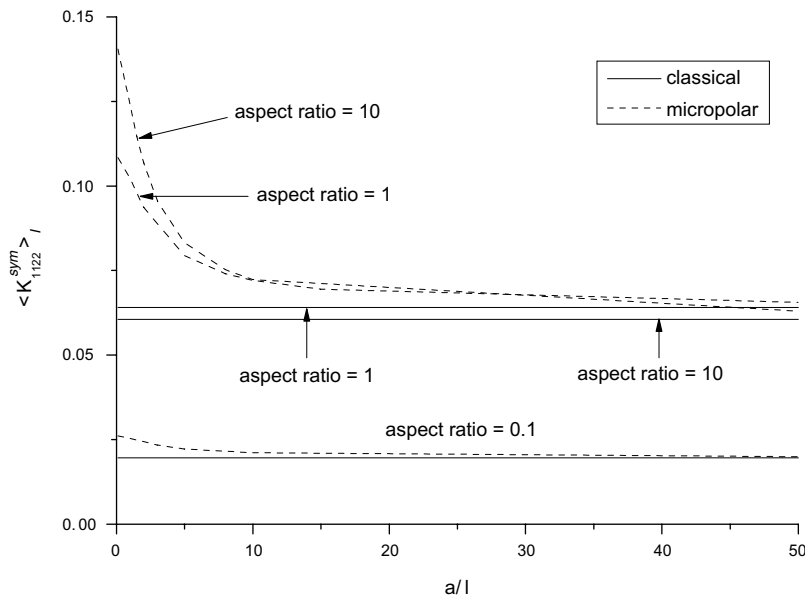


Fig. 6. Variation of component $\langle K_{1122}^{sym} \rangle / l$ of average Eshelby tensor as function of fiber size a for different aspect ratios 10, 1 and 0.1.

The variations of $\langle K_{1111}^{\text{sym}} \rangle_I$ and $\langle K_{1122}^{\text{sym}} \rangle_I$ of the average Eshelby tensor as function of inclusion's aspect ratio are shown in Figs. 3 and 4, respectively. For comparison the classical Eshelby tensor is also included. The exact values of the average Eshelby tensor for a spherical inclusion or cylindrical inclusion (Eq. (16)) are also included in the figures to access the accuracy of the numerical computation. The size of inclusion is set to be $a = l$. We found that our numerical results agree very well with the exact results in case of the spherical and cylindrical inclusion. For a cylindrical inclusion, there is a little difference between the numerical and the exact result, this is due to probably the finite aspect ratio used in the numerical computation.

The variations of the components $\langle K_{1111}^{\text{sym}} \rangle_I$ and $\langle K_{1122}^{\text{sym}} \rangle_I$ of the average Eshelby tensor as function of the size of inclusion are shown in Figs. 5 and 6, respectively. It is found that when the size of the inclusion approaches to the characteristic size of matrix material (l), the influence of inclusion size is more pronounced, and when the size of the inclusion is large enough, the micropolar Eshelby tensor is reduced to the classical one, as expected.

5. Conclusions

We therefore propose a method to evaluate the micropolar Eshelby tensors for a general ellipsoidal inclusion, and the analytical expressions of the four micropolar Eshelby tensors are derived, which involves only one-dimensional integral. The numerical computations of the Eshelby tensors are also performed, it is shown that the variation of the Eshelby tensors in an ellipsoidal inclusion is not significant, and when the size of the inclusion is large compared to the characteristic length of the material, the micropolar Eshelby tensor is reduced to the classical one.

Acknowledgement

This work is supported by the National Natural Science Foundation of China under Grants No. 10332020 and 10325210.

Appendix

The analytical expressions of Green's functions for a centrosymmetric and isotropic micropolar body have been derived by Sandru [10] and they are listed as follows:

$$G_{ln}(\mathbf{x} - \mathbf{x}') = G_{ln}^S(\mathbf{x} - \mathbf{x}') + \frac{H}{4\pi} \left[h^2 \left(\frac{e^{-r/h} - 1}{r} \right)_{,ln} - \delta_{ln} \frac{e^{-r/h}}{r} \right]$$

$$\Phi_{ln}(\mathbf{x} - \mathbf{x}') = \widehat{G}_{ln}(\mathbf{x} - \mathbf{x}') = \frac{1}{8\pi\mu} e_{lnk} \left(\frac{e^{-r/h} - 1}{r} \right)_{,k}$$

$$\widehat{\Phi}_{ln}(\mathbf{x} - \mathbf{x}') = -\frac{1}{16\pi\mu} \left(\frac{e^{-r/h} - 1}{r} \right)_{,ln} + \frac{1}{16\pi\kappa} \left(\frac{e^{-r/g} - e^{-r/h}}{r} \right)_{,ln} + \frac{\mu + \kappa}{16\pi\mu\kappa h^2} \delta_{ln} \frac{e^{-r/h}}{r}$$

where

$$r = |\mathbf{x} - \mathbf{x}'|, \quad H, g^2, h^2 \text{ are given by Eq. (9)}$$

$$G_{ln}^S(\mathbf{x} - \mathbf{x}') = \frac{1}{8\pi\mu} \left[2\delta_{ln} \frac{1}{r} - \frac{\lambda + \mu}{\lambda + 2\mu} r_{,ln} \right] \text{ is the classical Green's function.}$$

References

- [1] A.C. Eringen, *Microcontinuum Field Theories I: Foundations and Solids*, Springer Verlag, New York, 1999.
- [2] G.K. Hu, X.N. Liu, T.J. Lu, *Mech. Mater.* 37 (2005) 407–425.
- [3] R.S. Lakes, *J. Mater. Sci.* 18 (1983) 2572–2581.
- [4] Z.Q. Cheng, L.H. He, *Int. J. Eng. Sci.* 33 (1995) 389–397.

- [5] Z.Q. Cheng, L.H. He, *Int. J. Eng. Sci.* 35 (1997) 659–668.
- [6] J.D. Eshelby, *Proc. R. Soc. London, A* 241 (1957) 376–396.
- [7] F. Xun, G.K. Hu, Z.P. Huang, *Int. J. Solids Struct.* 41 (2004) 4713–4730.
- [8] X.N. Liu, G.K. Hu, *Int. J. Plast.* 21 (2005) 777–799.
- [9] W. Nowacki, *Theory of Asymmetric Elasticity*, Pergamon press, 1986.
- [10] N. Sandru, *Int. J. Eng. Sci.* 4 (1966) 81–96.
- [11] T. Mura, *Micromechanics of Defects in Solids*, Martinus Nijhoff, Netherlands, 1982.
- [12] T.M. Michelitsch, H. Gao, V.M. Levin, *Proc. R. Soc. London, A* 459 (2003) 863–890.